Ministry of Science and Higher Education
Republic of Poland

Jagiellonian University in Kraków

European Space Agency

Dispersive Ionospheric Phase Estimation in L-band InSAR Using Fourier Neural Operators

Kazuki Yanagiya, Yutaro Shigemitsu, Takeshi Motohka, Takeo Tadono

Earth Observation Research Center, Japan Aerospace Exploration Agency

16 June 2026

Northern Lights at Old Crow, Yukon

Background

- **Ionospheric path delay phase** is a major phase component in InSAR, particularly in long-wavelength L-band SAR systems (e.g., Rosen et al., 2010; Meyer, 2011).
- Accurate estimation and correction of the ionospheric path delay phase are essential for precise retrieval of ground deformation.

ALOS-2 (10 m) NE-Siberia
2024/9/22 – 2024/10/6

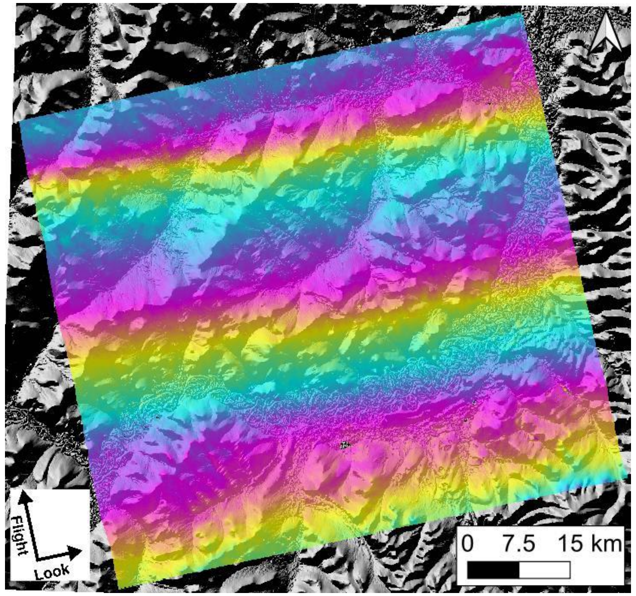

ALOS-2 (10 m) North of Fairbanks
2022/8/19 – 2023/8/18

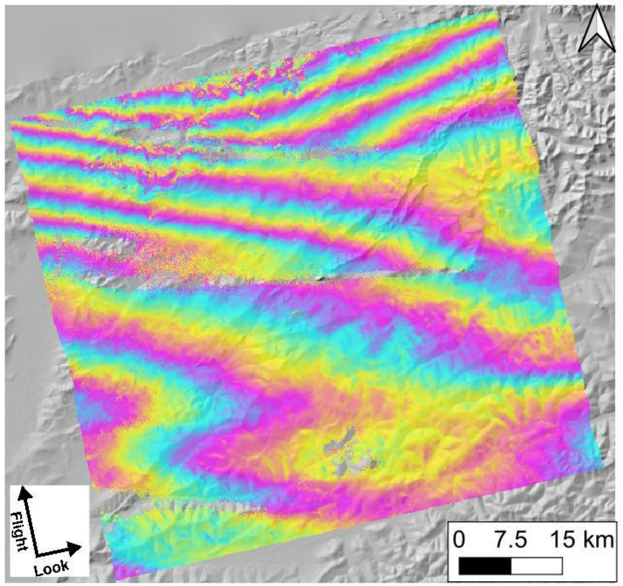

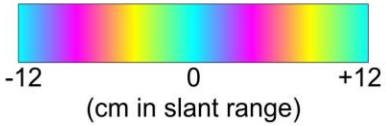

ALOS-2 (3 m) Yukon
2023/6/13 – 2023/7/11

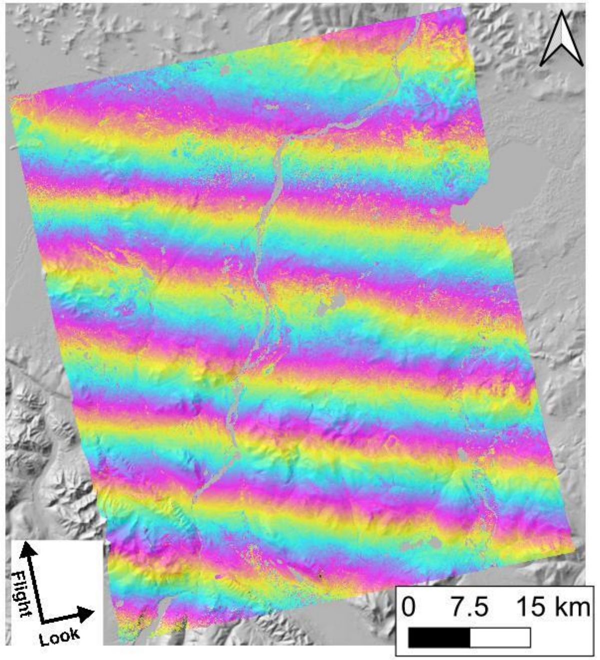

Ionospheric Correction with Split Spectrum Method (SSM)

- SSM separates ionospheric path delay phase from sub-band interferograms using its frequency dependence (e.g., Gomba et al., 2016).

$$\Delta\phi = \frac{4\pi f_0}{c}(\Delta r_{\text{topo}} + \Delta r_{\text{mov}} + \Delta r_{\text{tropo}}) - \frac{4\pi K}{c f_0}\Delta\text{TEC}$$

- In practice, **pre- and post-smoothing** are often required to suppress unwrap error, decorrelation, and misregistration noise.

- Various improved methods have been proposed to achieve more accurate ionospheric estimates under noisy conditions.

  Reformulating the estimation equation (Wegmüller et al., 2018)

  Time-series-based inverse estimation (Mao et al., 2023)

  Polynomial fitting combined with Gaussian smoothing (Nagaoka et al., 2025)

Low-band interferogram $\Delta\phi_L$

High-band interferogram $\Delta\phi_H$

Can deep learning model the full SSM process, including smoothing?

Ionospheric phase $\Delta\hat{\phi}_{iono}$

Noto, Japan

Training and Inference Framework

The deep learning model is trained on simulated data by minimizing the loss between estimated and reference ionospheric phases.

The trained model is then applied to real interferograms to estimate the ionospheric phase.

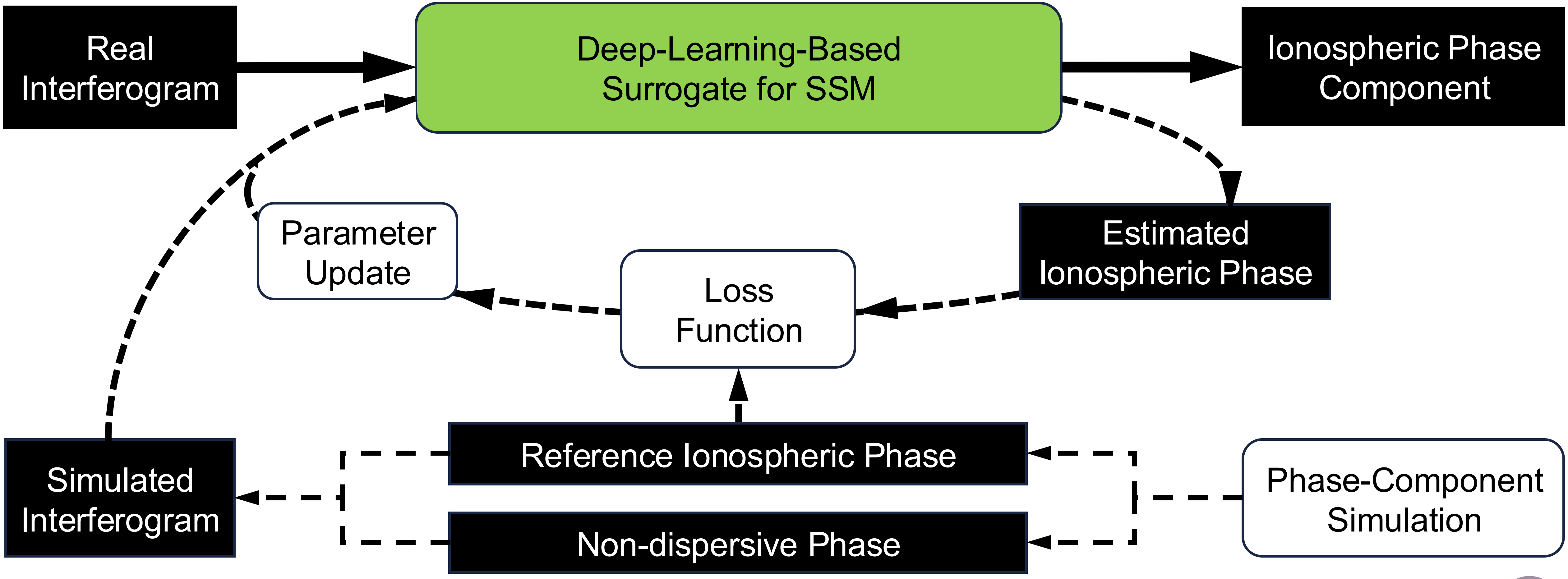

From Neural Networks to Operator Learning

- **Neural networks** with enough hidden units can approximate a wide variety of complex functions with arbitrary accuracy (Hornik et al., 1989).
- However, they are not primarily designed to directly learn operators on continuous function spaces, and the approximation ability does **not guarantee good generalization to unseen inputs**.
- **Neural operators** are a generalization of neural networks that can learn operators: mappings between two functions (or fields) defined on continuous domains (Azizzadenesheli et al., *Nat. Rev. Phys.*, 2024).

Classical neural network: vector-to-vector mapping

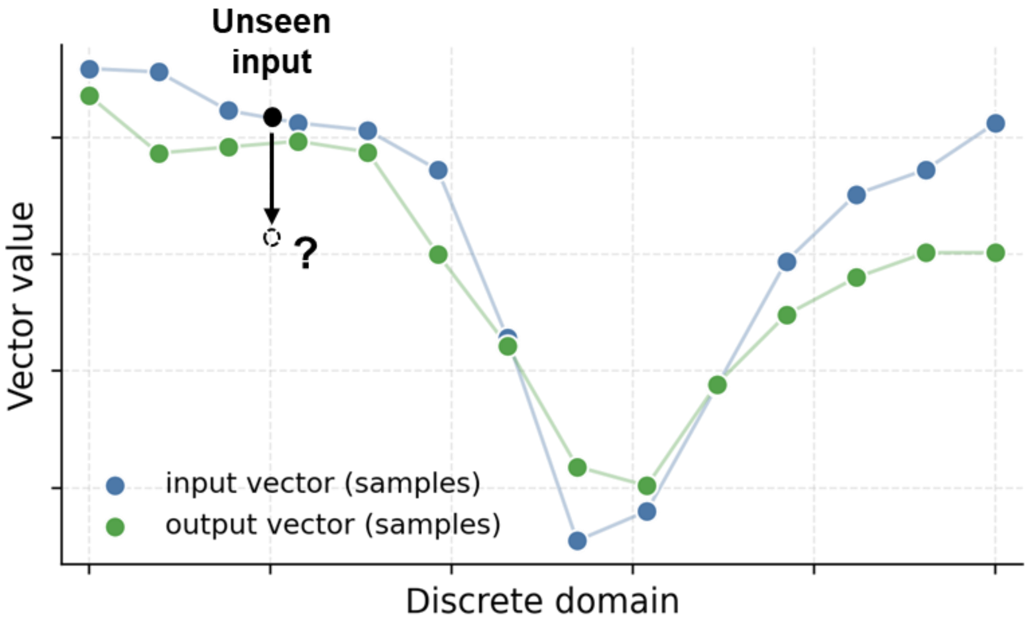

Neural operator: function-to-function mapping

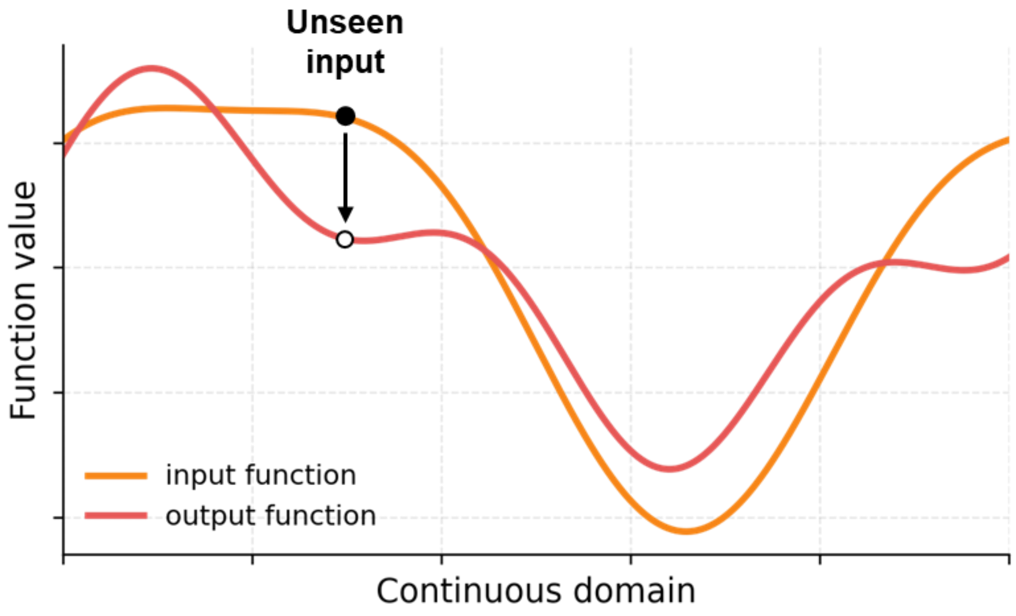

What is a Fourier Neural Operator (FNO)?

- FNO is a neural operator that uses **Fourier transforms** to model operators between functions (Li et al., 2021; Kovachki et al., 2021).
- It was originally proposed as a **fast surrogate model for PDE-based simulations** and is now increasingly used for this purpose.
- Instead of solving equations iteratively, FNO directly predicts the output field from the input field after training.

Zero-shot super-resolution: Navier-Stokes Equation with viscosity v = 1e− 4

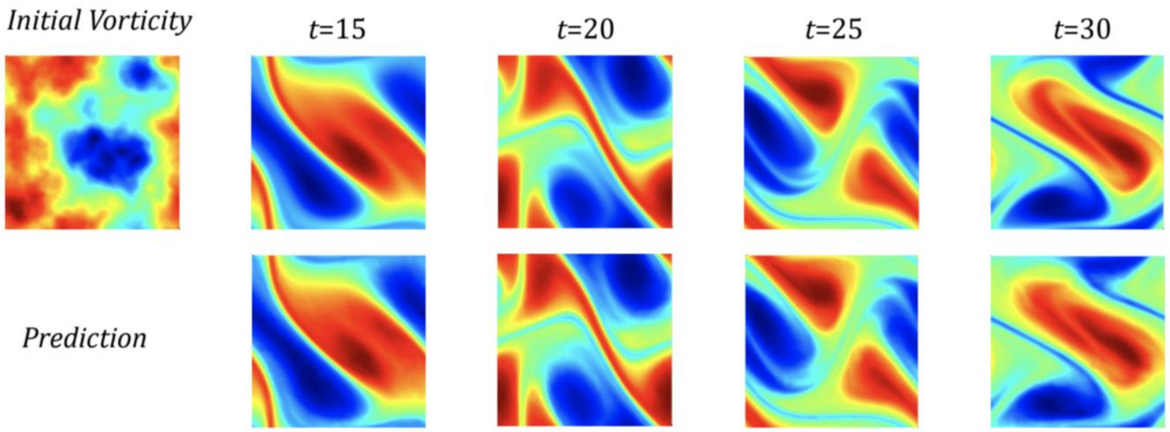

(Li et al., 2021)

Surface windspeed predictions with Spherical FNO and ground truth data (NVIDIA)

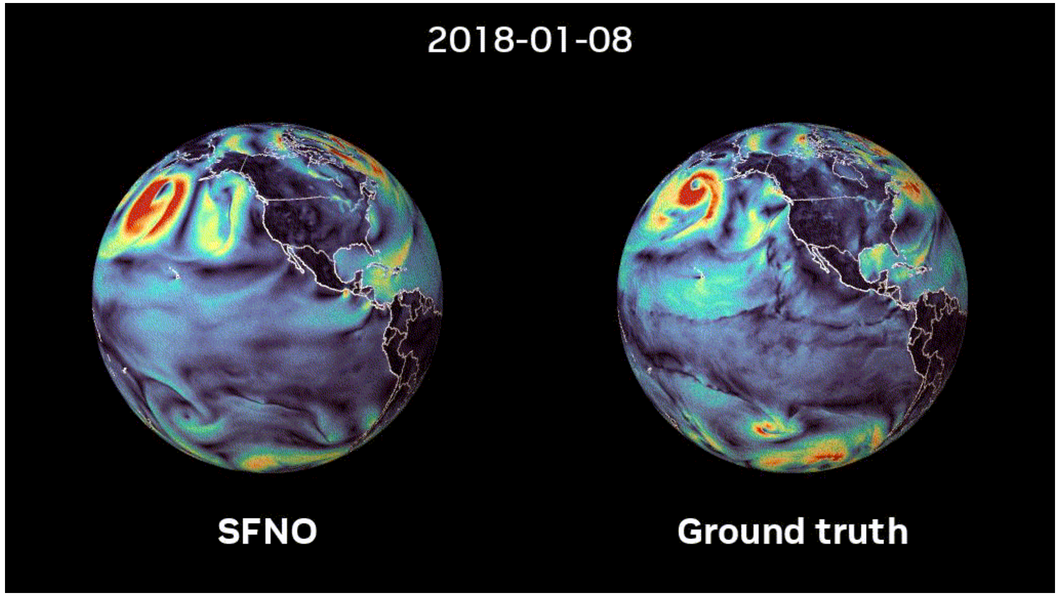

(https://developer.nvidia.com/blog/modeling-earths-atmosphere-with-spherical-fourier-neural-operators/)

FNO Principle

Learn a parametric operator ($\mathcal{G}_\theta$) that maps the input function space ($\mathcal{A}$) to the output function space ($\mathcal{U}$) (Li et al., 2021; Kovachki et al., 2021).

Schematic of the FNO model

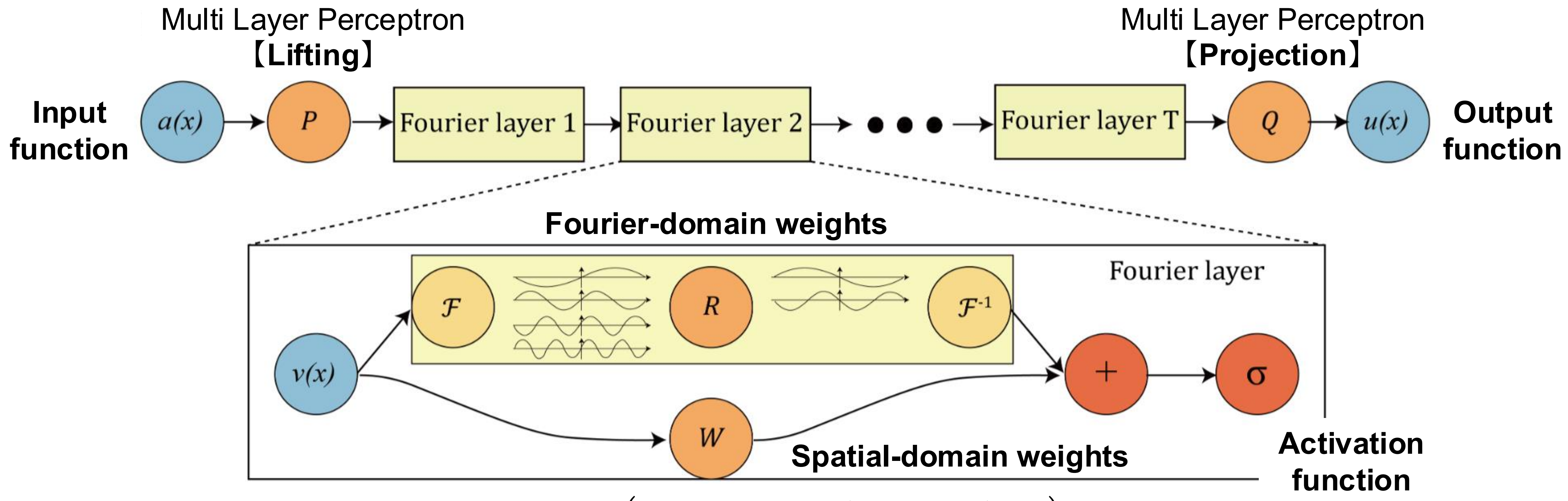

$$v_{t+1}(x) = \sigma\left(W_t v_t(x) + \mathcal{F}^{-1}\left(R_\phi \cdot (\mathcal{F} v_t)\right)(x)\right)$$

(Modified from Li et al., 2021)

Proposed Learning Framework

We used FNO to map noisy unwrapped sub-band phases to a noise-free unwrapped ionospheric phase.

The spatial size (m × n) remains unchanged throughout the entire process from input to output.

➡ The model can handle data with different spatial sizes at inference time.

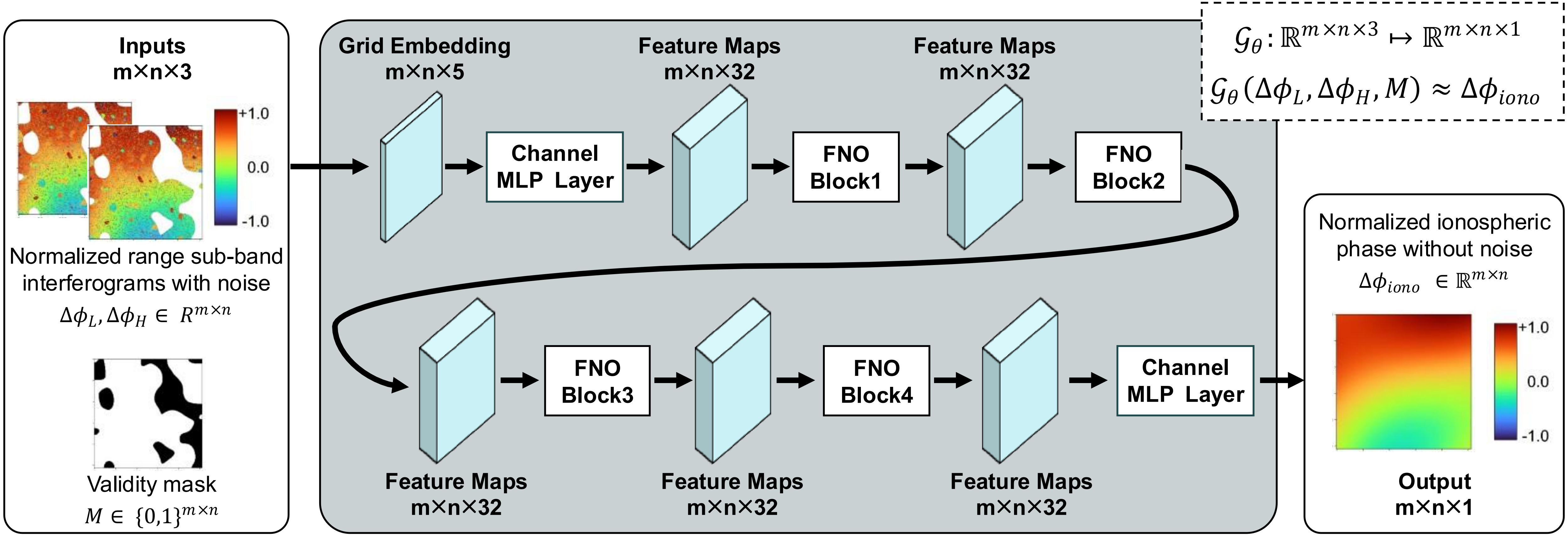

(Yanagiya et al., 2026)

Training Environment

Training and evaluation were conducted on a shared GPU workstation (NVIDIA GeForce RTX 5090, 32 GB VRAM).

All training, validation, and test data consisted of simulated interferograms generated with a modified method based on previous studies (Ebmeier, 2016; Anantrasirichai et al., 2019).

- Rapid generation of large ground-truth datasets without manual labeling
- Potential performance limitations due to the simulation-to-reality gap

Experimental Settings

Implementation	neuraloperator library with PyTorch https://github.com/neuraloperator/neuraloperator (Kossaifi et al., 2024)
Training data	100,000 simulated images
Validation data	25,000 simulated images
Test data	10,000 simulated images
Image size	256×256 pixels
Loss function	Weighted MSE Weight: 0.01 for masked pixels, 1.0 otherwise
Optimizer	AdamW (Loshchilov and Hutter, 2019)
Initial learning rate	10^{-3}
Weight decay	5×10^{-3} for regularization
Scheduler	Cosine annealing
Training epochs	100 epochs

Generation of simulated interferograms: : Nondispersive phase

$$\Delta\phi_{int} = \Delta\phi_{def} + \Delta\phi_{turb} + \Delta\phi_{strat} + \Delta\phi_{trend} + \Delta\phi_{iono} + \Delta\phi_{err}$$

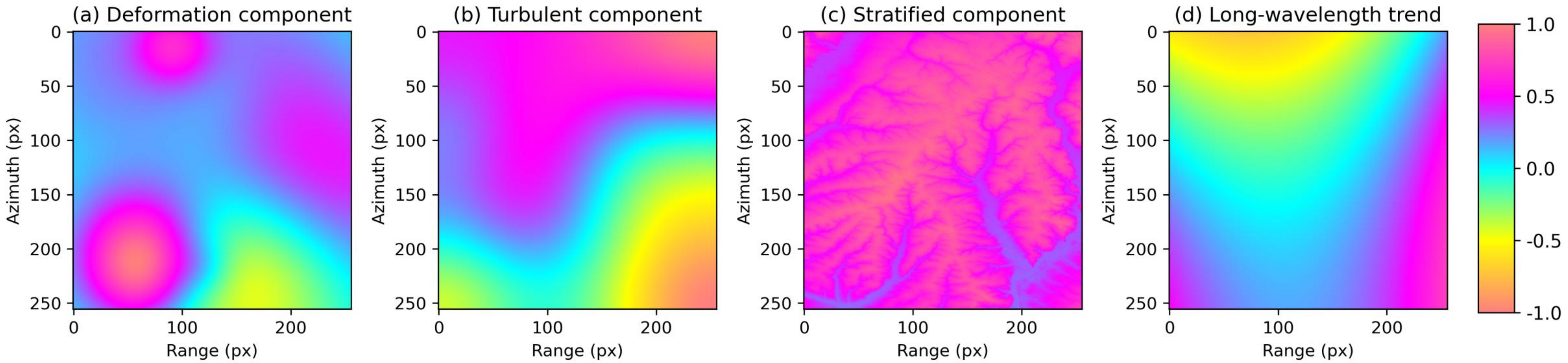

Component	Simulation Method
$\Delta\phi_{disp}$	Superposition of spatially correlated Gaussian patches
$\Delta\phi_{turb}$	Spatially correlated phase variations generated from Gaussian noise and Gaussian filtering
$\Delta\phi_{strat}$	Elevation-dependent component derived from the AW3D30 digital elevation model
$\Delta\phi_{trend}$	Quadratic polynomial

(Yanagiya et al., 2026)

Generation of simulated interferograms : Dispersive phase

$$\Delta\phi_{int} = \Delta\phi_{def} + \Delta\phi_{turb} + \Delta\phi_{strat} + \Delta\phi_{trend} + \Delta\phi_{iono} + \Delta\phi_{err}$$

The TEC field was modeled as the sum of a stable background and a spatially heterogeneous anomaly component.

The anomaly component was simulated as a superposition of plane waves, following the ocean-wave simulation approach of Tessendorf (2001).

$$TEC_{anom}(x,y) = \sum_{i}^{N} A_i \, cos\left(k_{xi}x + k_{yi}y + \phi_i\right)$$

Wavelengths were randomly chosen from **100 to 1000 km**, following typical MSTID/LSTID scales (Otsuka et al., 2013; Tsugawa et al., 2004).

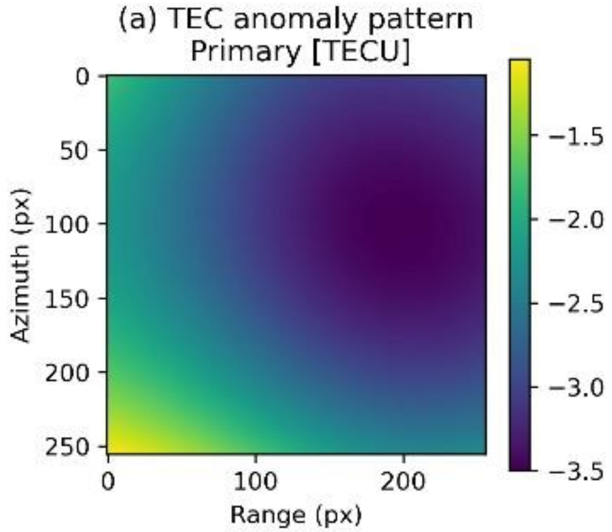

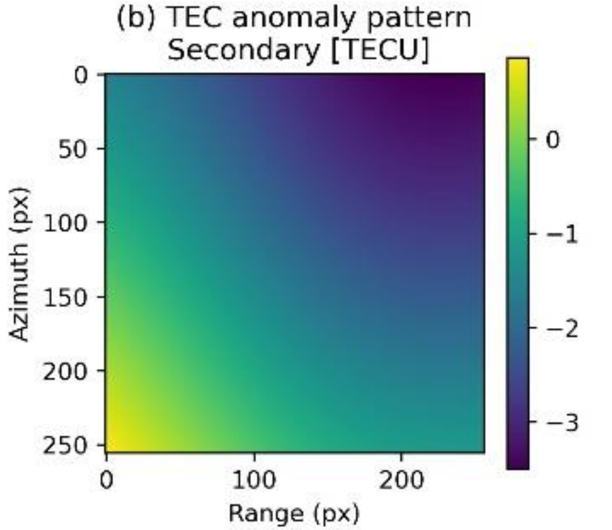

(Yanagiya et al., 2026)

Generation of simulated interferograms: Dispersive phase

$$\Delta\phi_{int} = \Delta\phi_{def} + \Delta\phi_{turb} + \Delta\phi_{strat} + \Delta\phi_{trend} + \Delta\phi_{iono} + \Delta\phi_{err}$$

The heterogeneous component was normalized to [-1,1] and scaled to a representative GNSS-derived amplitude of 3.5 TECU (Pi et al., 2021).

Assuming a temporally uniform background component, the TEC difference was defined from the difference between the anomaly fields.

$$\Delta TEC(x,y) = A_{anom}\left(TEC^{norm}_{anom,sec} - TEC^{norm}_{anom,pri}\right)$$

The ionospheric path delay phase was then generated from the simulated TEC difference using Eq. (4) in Gomba et al. (2016).

$$\Delta\phi_{iono}(x,y) = -\frac{4\pi K}{c f_0}\Delta TEC(x,y)$$

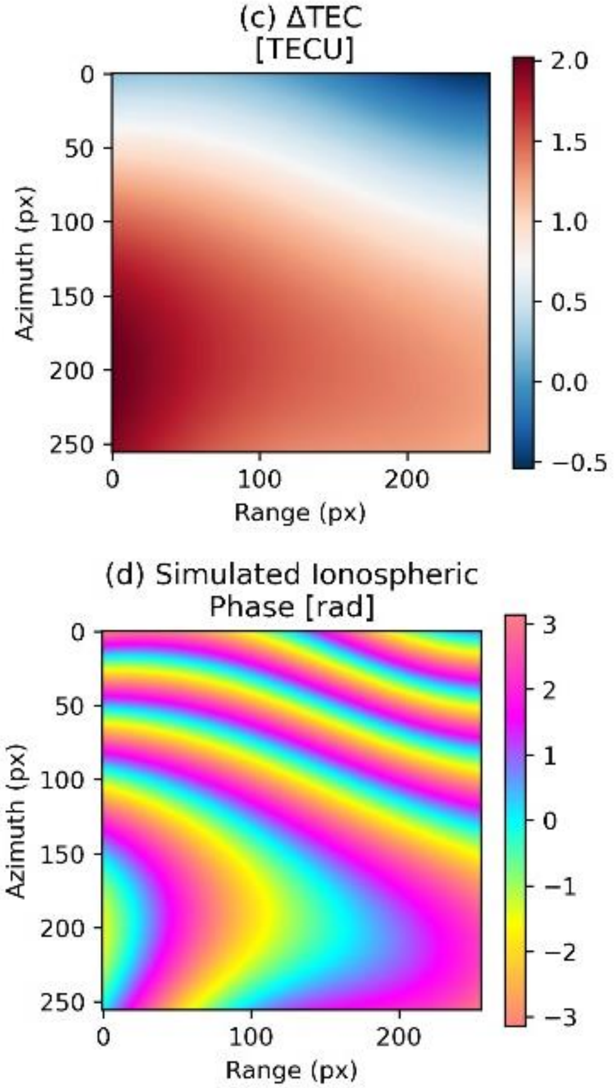

(Yanagiya et al., 2026)

Generation of simulated interferograms

We combined the phase components with random weights to generate synthetic high- and low-band interferometric phases.

The simulated interferograms were normalized to [-1, 1].

$f_0 = 1.25750$ GHz, $f_L = 1.25283$ GHz, $f_H = 1.26216$ GHz
The frequency difference $\Delta f = 9.33$ MHz

We then added, over 0–80% of the image area:
a. Random offsets to mimic local unwrapping errors
b. Random noise for each pixel
c. No-data areas

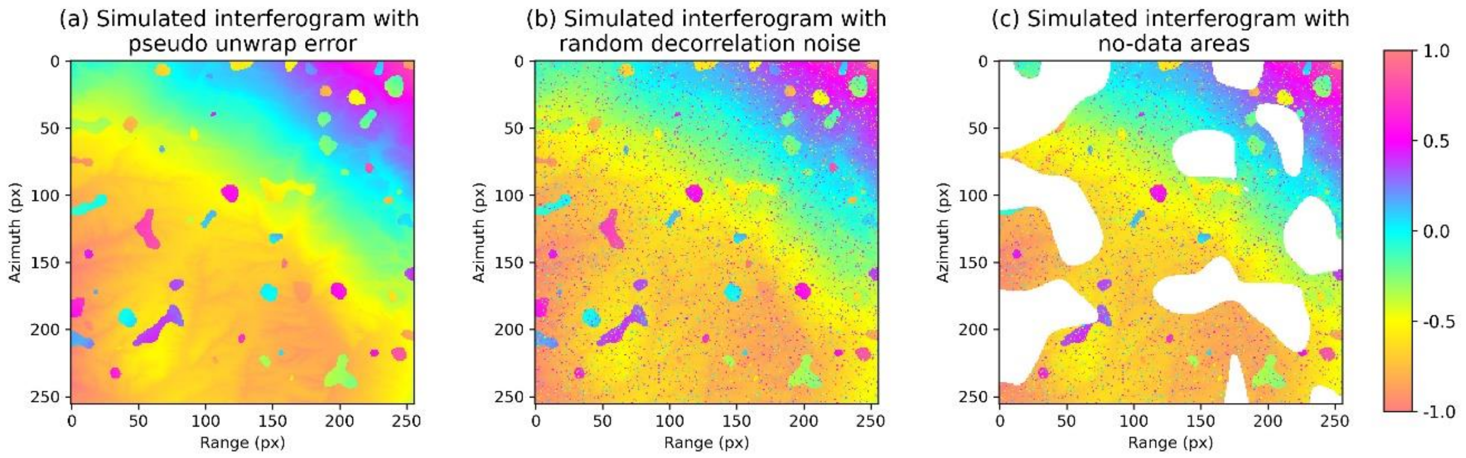

(Yanagiya et al., 2026)

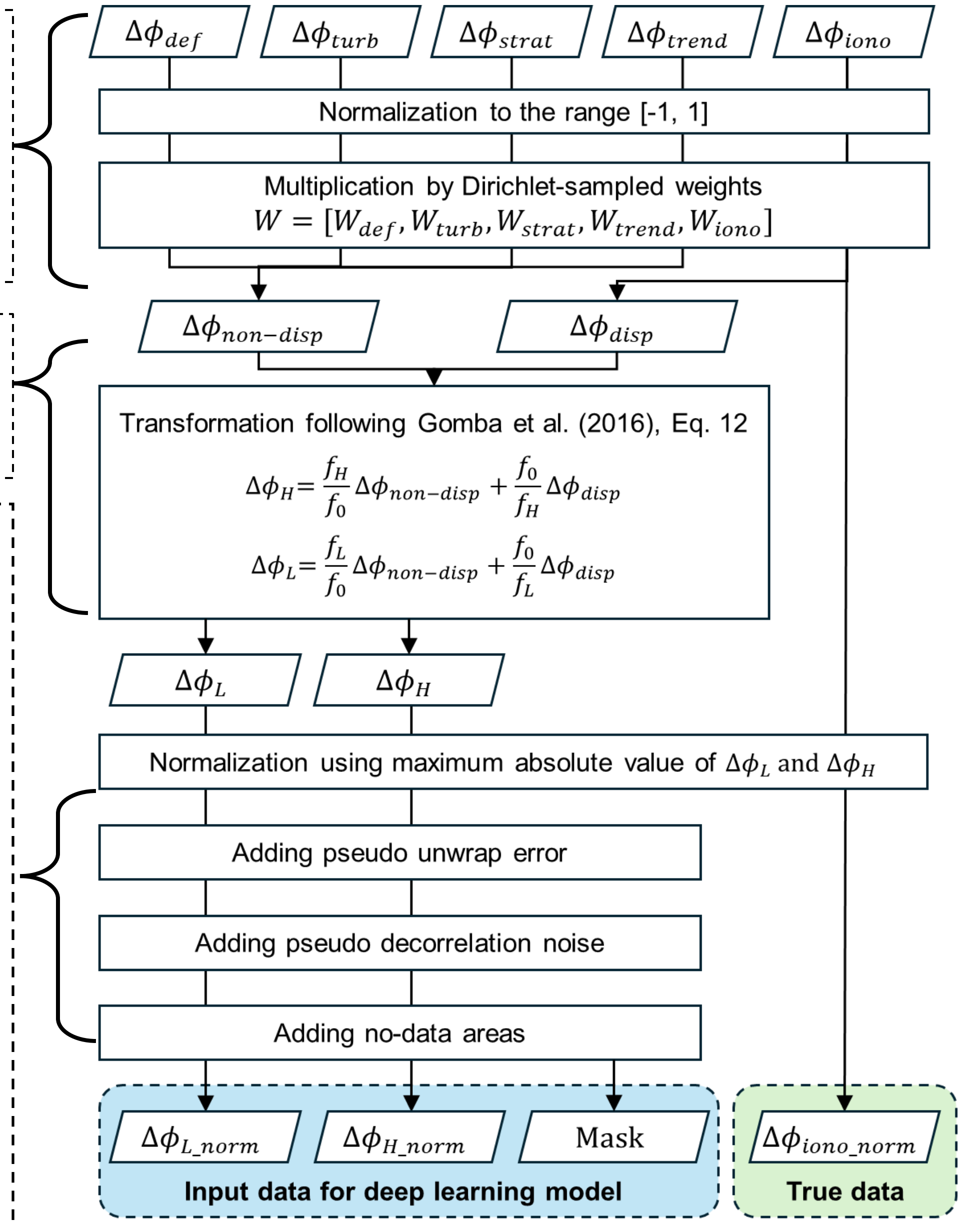

Loss curves & Test data inference

- Both training and validation MSE losses decreased and converged to similar values over 100 epochs.
- Training for 100 epochs with a batch size of 64 took about 8 hours.

The final training MSE loss:	0.000039
The final validation MSE loss:	0.000046

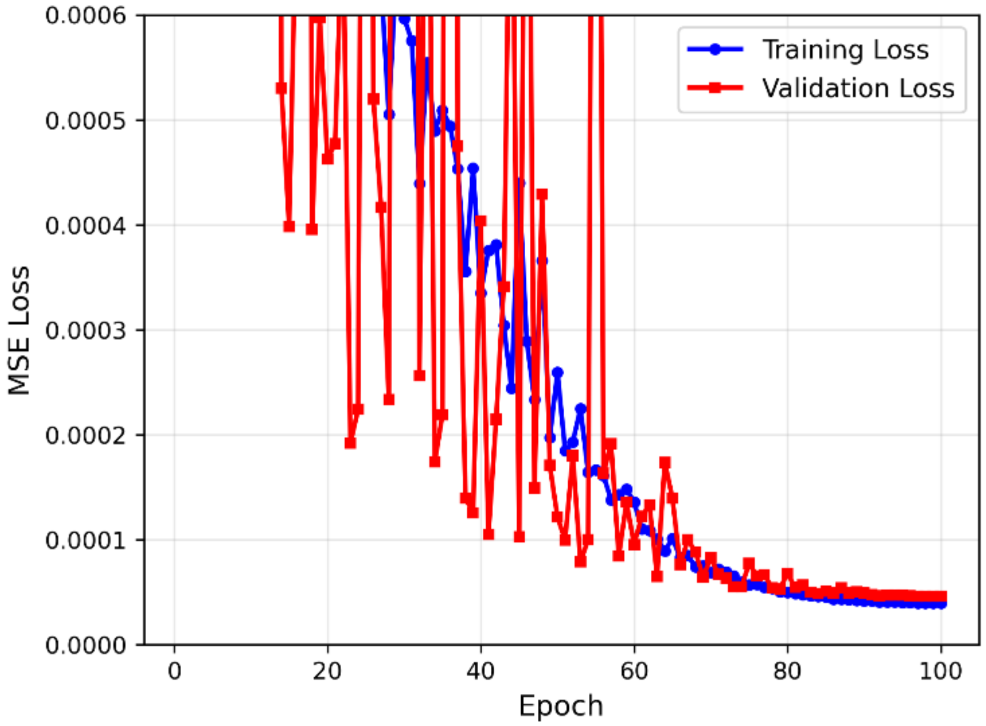

- The proposed FNO accurately estimated the ionospheric path delay phase on 10,000 unseen synthetic interferograms.

	Over valid pixels	Over all pixels
RMSE	0.0073±0.0089	0.0146±0.0368
SSIM	0.988±0.025	0.956±0.099

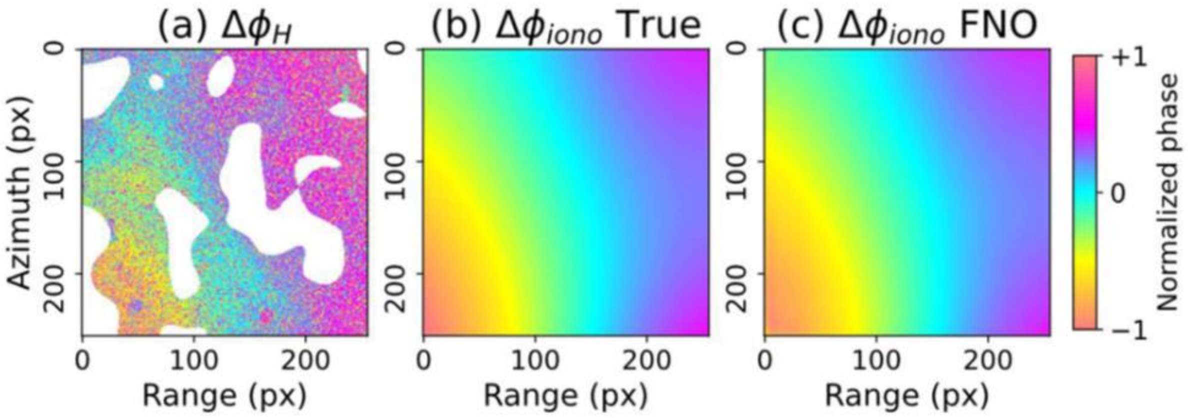

(Yanagiya et al., 2026)

Evaluation of generalization across spatial sizes

Using a model trained on 256 × 256 data, we evaluated the inference accuracy on inputs ranging from 32 × 32 to 2048 × 2048.

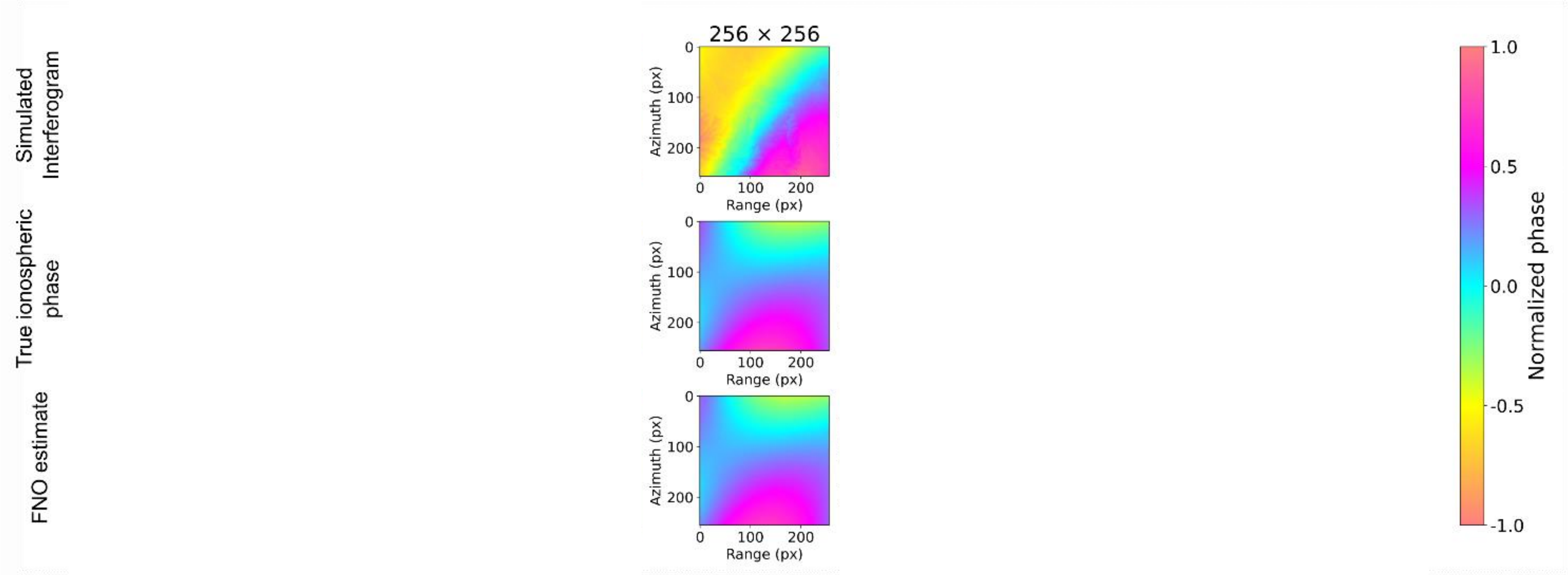

(Yanagiya et al., 2026)

Validation against theoretical values

We tested the model with scalar inputs and compared the outputs with the values derived from the theoretical formula.

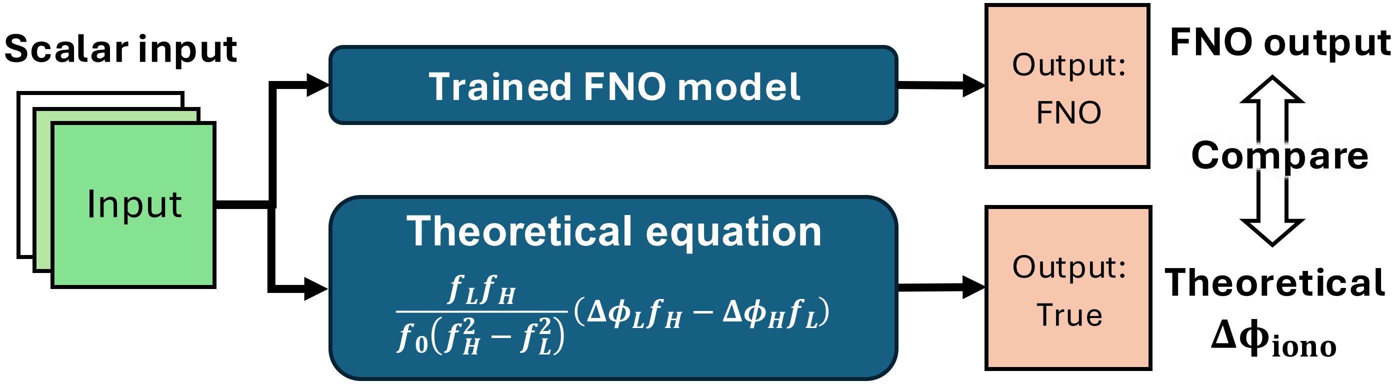

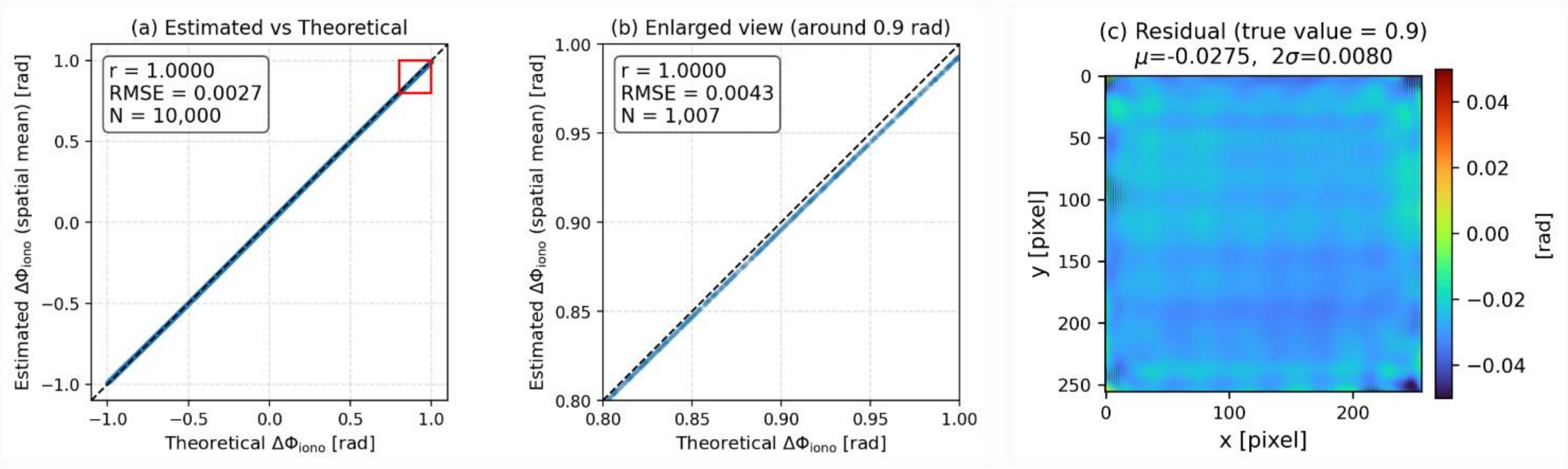

(Yanagiya et al., 2026)

Validation of inference using ALOS-2 data

FNO-based inference was evaluated using three ALOS-2 interferograms with different geographic conditions, spatial sizes, and coherence levels.

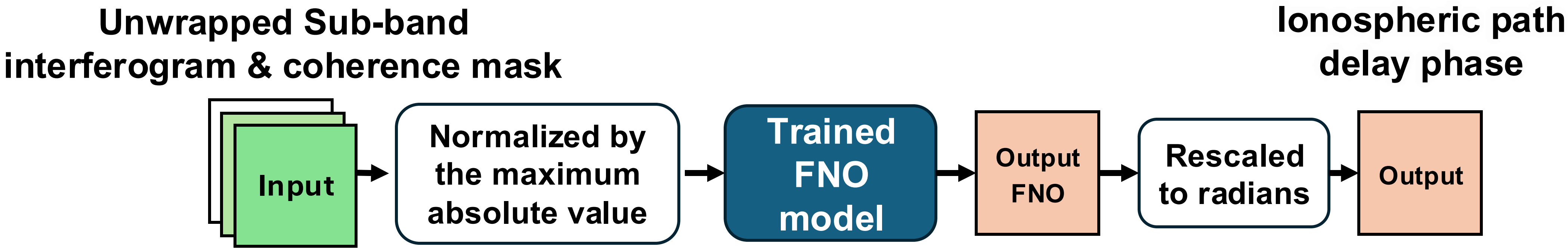

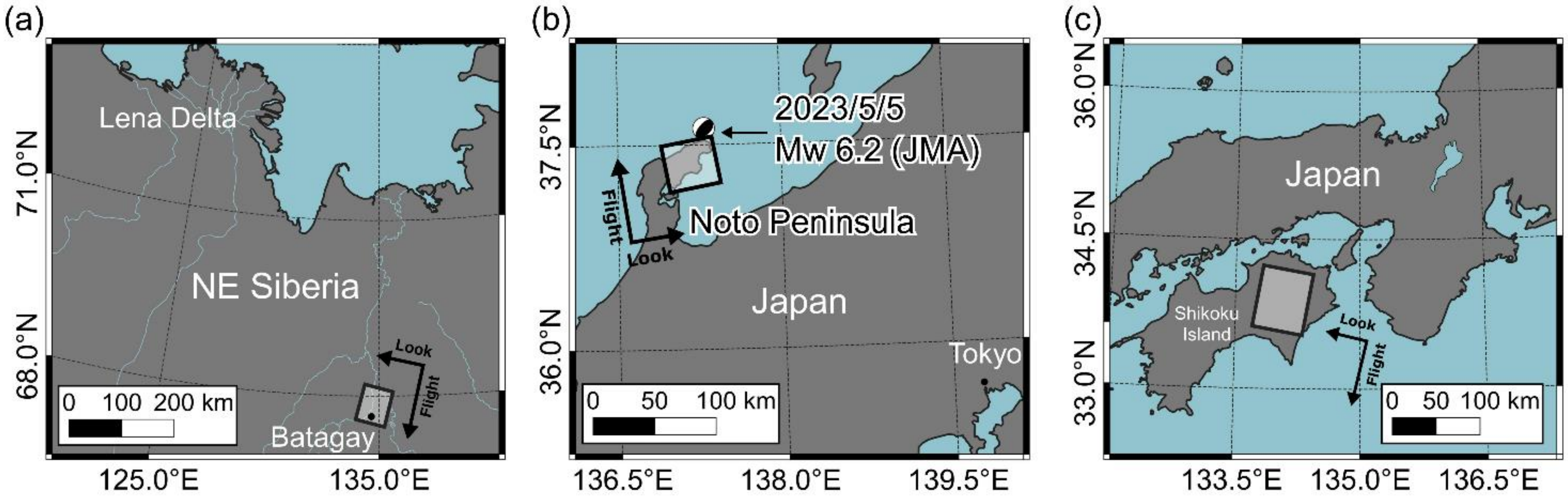

(Yanagiya et al., 2026)

Validation of inference using ALOS-2 data

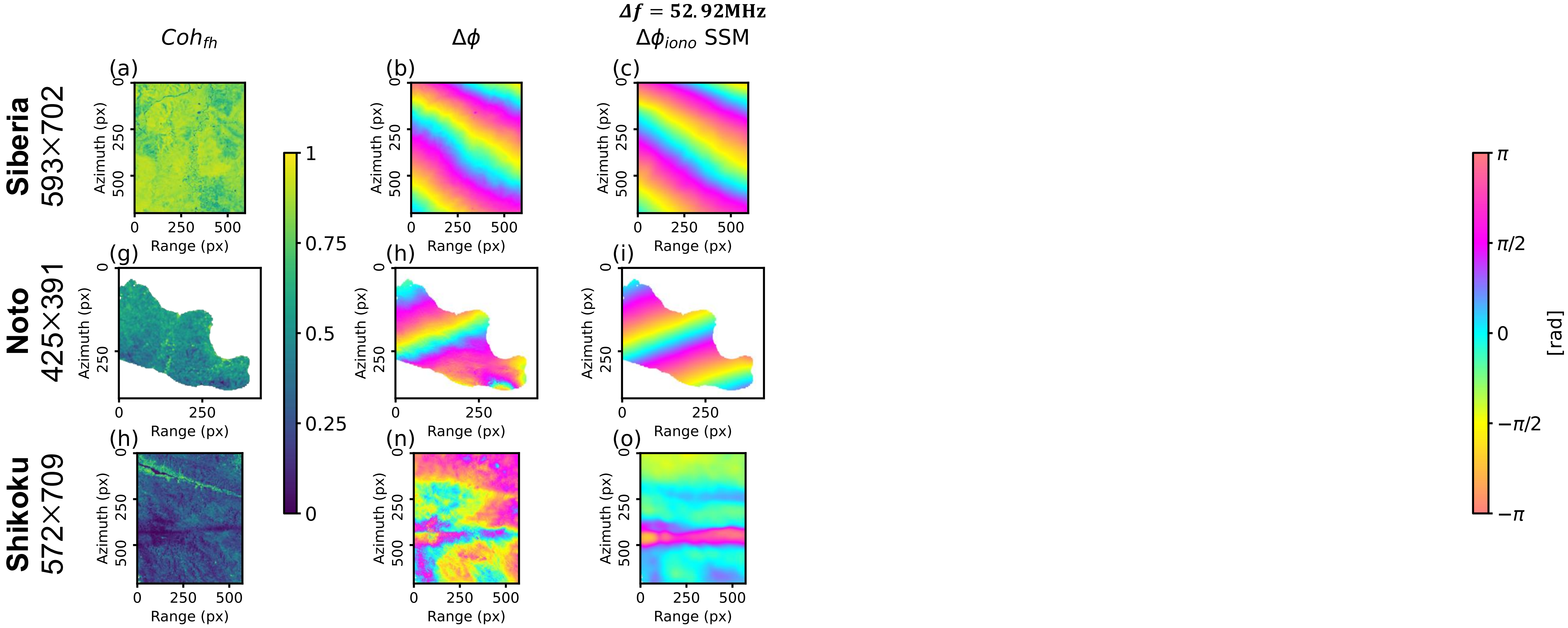

(Yanagiya et al., 2026)

The Shikoku case included a localized ionospheric disturbance with a spatial scale of about **10 km**, reported as sporadicE by Fujimoto et al. (2024). This scale is far smaller than the **100–1000 km** range simulated in this study and is considered a major cause of the degraded estimation accuracy.

Model update: frequency information as an input feature

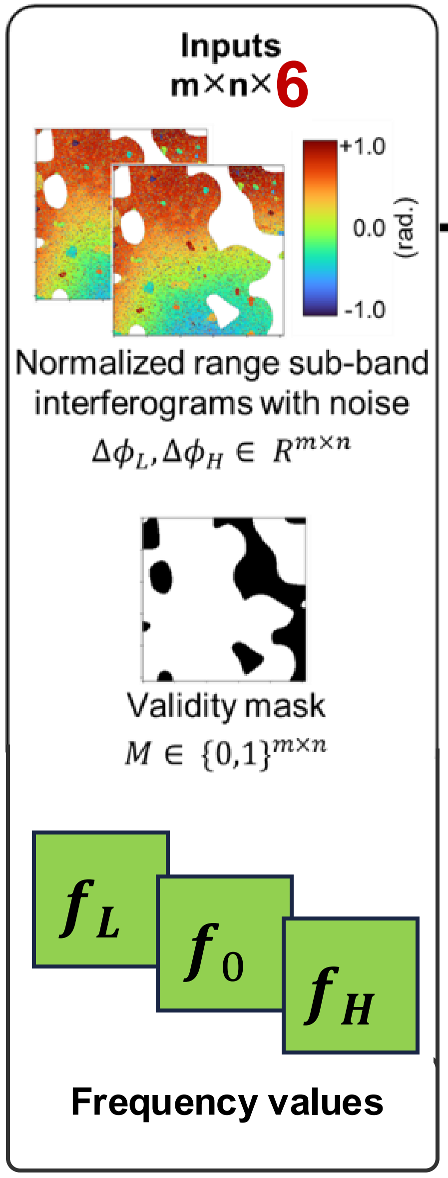

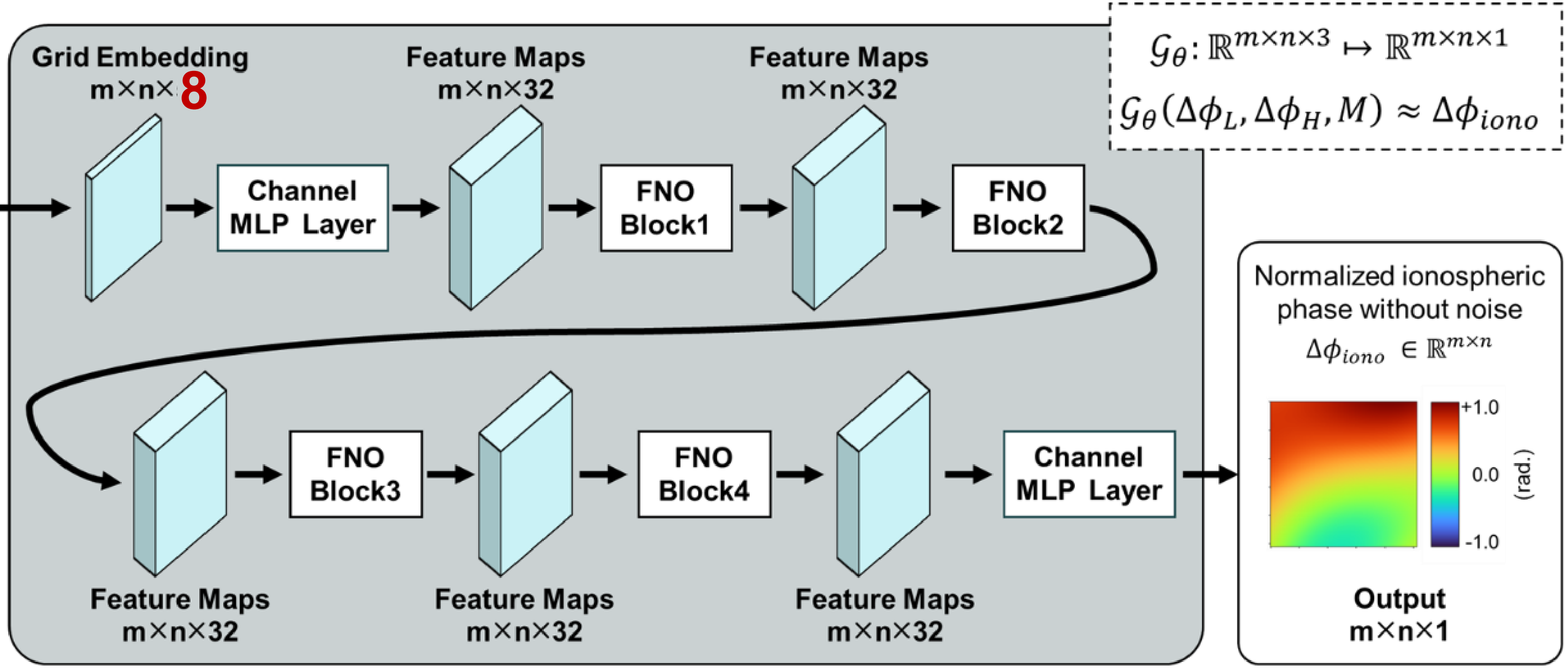

Previous model: Fixed input frequency conditions

Improved model: Supports arbitrary frequency conditions by explicitly taking frequency values as input

Preliminary results of the frequency-input model: NISAR

NISAR pre-calibration data (Ethiopia) 2025/11/22 – 2025/12/24

L1 RSLC, L-band, Ascending, Left-looking, HH

1.2290 GHz center frequency; 20 MHz bandwidth

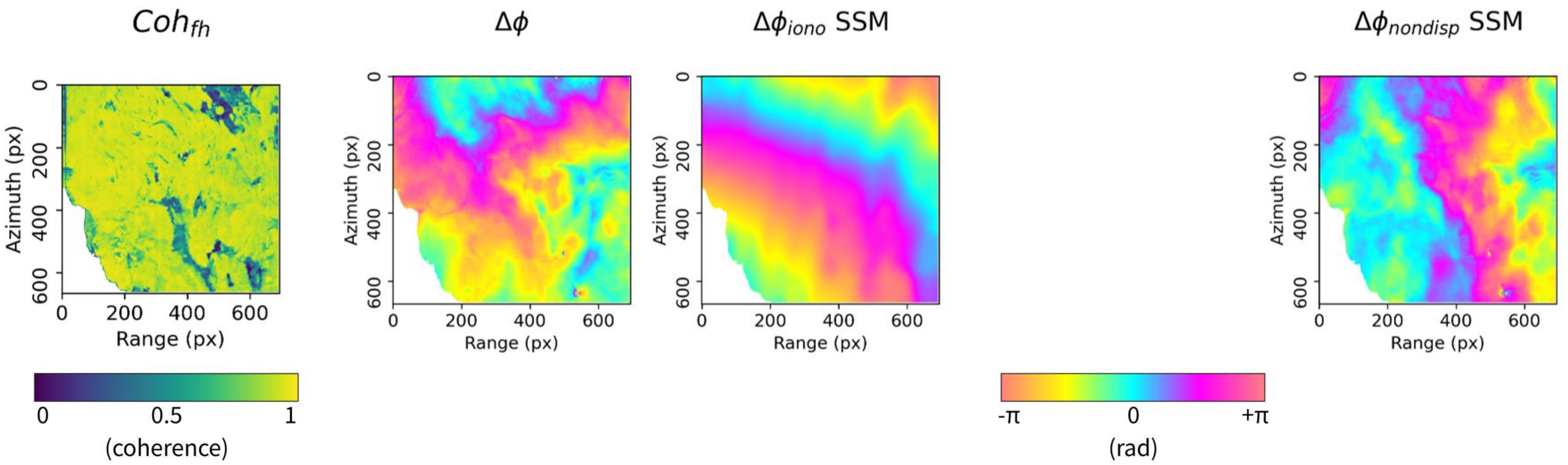

By providing frequency information as an additional input, the model can also be applied to data acquired under different frequency conditions.

ALOS-2 ScanSAR data (Mackenzie Delta, Canada) 2025/08/04 - 2025/09/01

Ascending, Right-looking, HH, 1.2365 GHz center frequency; 11.9 MHz bandwidth

Azimuth streaks were corrected using pixel offsets, but some residuals remain in the lower part of the image.

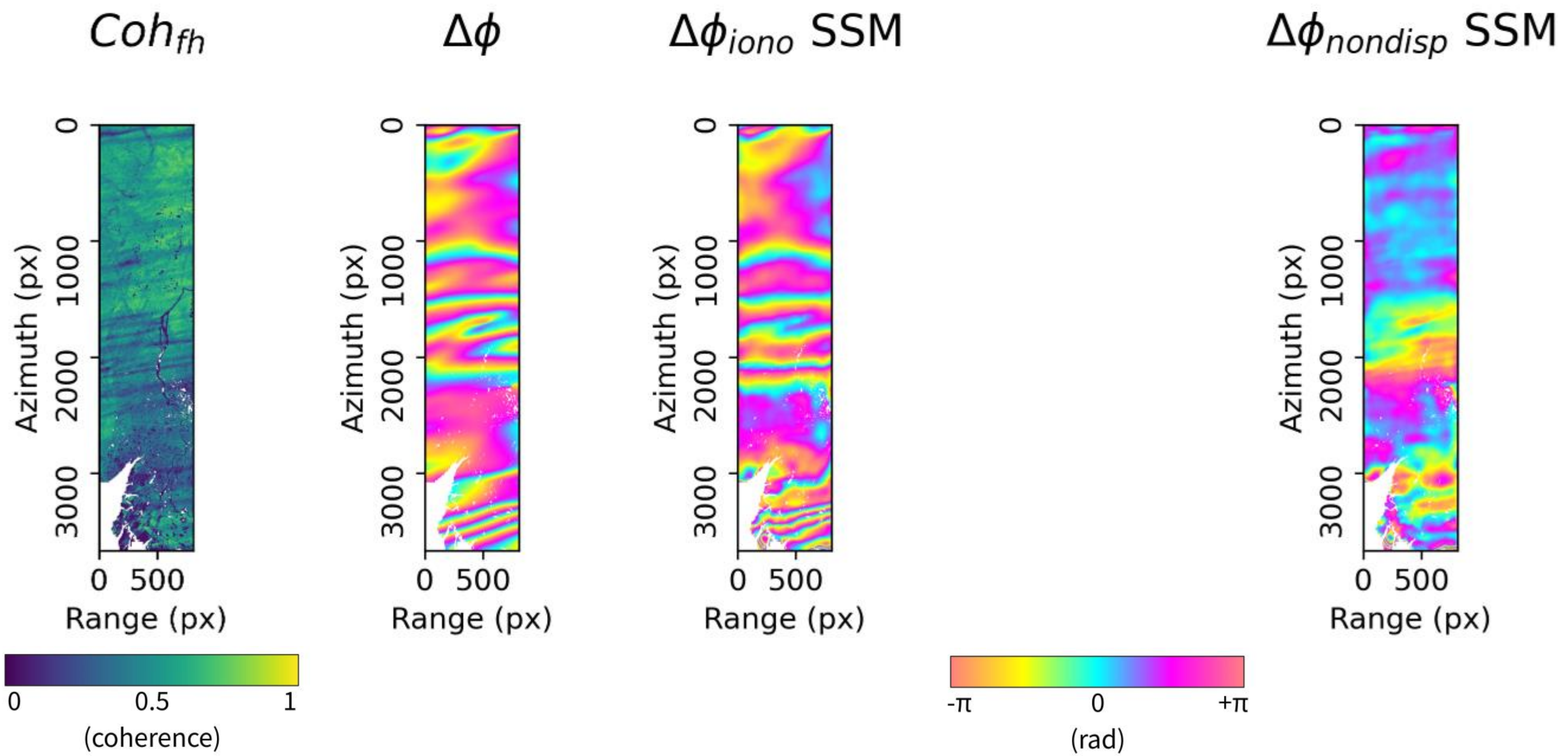

Summary

- The FNO surrogate learned both spatial patterns and the SSM-based relationship, and generalized from simulated to real ALOS-2 and NISAR data without retraining.
- However, performance degraded for unseen localized ionospheric disturbances (e.g., sporadic-E, azimuth streaks).

	SSM	FNO surrogate for SSM
Separation criterion	Frequency dispersion	Learned spatial patterns & Frequency dispersion
Range sub-band	Two sub bands	Two sub bands
Training data	Not required	**Required**; **simulated data can be used**
Strengths	Physically interpretable	**Potential robustness to noise and missing data**
Weaknesses	Sensitive to narrow bandwidth and low coherence	**Depends on training data, setup, and generalization**

- **Future work:** physics-constrained models, local-structure simulation, and advanced models (e.g., U-FNO and Local-FNO).

Thank you for your attention.

Poster Session1 (Tuesday, 16/June/2026: 4:30pm - 7:00pm)

Y. Shigemitsu et al., Theory-consistent Interpretation of ICA Decomposed InSAR Sources: DEM Error and Ionospheric Delay

The first part of this study has been published in IEEE GRSL.

IEEE GEOSCIENCE AND REMOTE SENSING LETTERS, VOL. 23, 2026 4008805

Fourier Neural Operator Approach for Ionospheric Phase Compensation in L-Band SAR Interferometry

Kazuki Yanagiya, *Member, IEEE*, Yutaro Shigemitsu, *Member, IEEE*, Takeshi Motohka, *Member, IEEE*, and Takeo Tadono, *Member, IEEE*

***Abstract*—The ionosphere introduces path delay phases into interferometric synthetic aperture radar (InSAR) images, degrading the accuracy of ground deformation measurements particularly for long-wavelength L-band systems. Analytical split-**

spectrum method (SSM) exploits the distinct frequency dependence of nondispersive and dispersive phase components to analytically estimate ionospheric phase from range sub-band interferograms [3]. In practice, the L-band bandwidth (e.g.,

You can access it here: